

Time Dependent Theory for Random Lasers

Xunya Jiang and C. M. Soukoulis

Ames Laboratory—USDOE and Department of Physics and Astronomy, Iowa State University, Ames, Iowa 50011
(Received 3 December 1999)

A model to simulate the phenomenon of random lasing is presented. It couples Maxwell's equations with the rate equations of electronic population in a disordered system. Finite difference time domain methods are used to obtain the field pattern and the spectra of localized lasing modes inside the system. A critical pumping rate P_r^c exists for the appearance of the lasing peaks. The number of lasing modes increases with the pumping rate and the length of the system. There is a lasing mode repulsion. This property leads to a saturation of the number of modes for a given size system and a relation between the localization length ξ and average mode length L_m .

PACS numbers: 42.55.-f, 05.40.-a, 42.25.Bs, 72.15.Rn

The interplay of localization and amplification is an old and interesting topic in physics research [1]. With promising properties, mirrorless random laser systems are widely studied [2–7] both experimentally and theoretically. Recently, new observations [2] of laserlike emission were reported and showed new interesting properties of amplifying media with strong randomness. First, sharp lasing peaks appear when the gain or the length of the system is over a well-defined threshold value. Although a drastic spectral narrowing has been previously observed [3], discrete lasing modes were missing. Second, more peaks appear when the gain or the system size further increases over the threshold. Third, the spectra of the lasing system is direction dependent, not isotropic. To fully explain such an unusual behavior of stimulated emission in random systems with gain, we are in need of new theoretical ideas.

Based on the time-dependent diffusion equation, earlier work of Letokhov [1] predicted the possibility of lasing in a random system and Zyuzin [5] discussed the fluctuation properties near the lasing threshold. Recently, John and Pang [6] studied the random lasing system by combining the electron number equations of energy levels with the diffusion equation. By using the diffusion approach, it is not possible to explain the lasing peaks observed in the recent experiments [2] in both semiconductor powders and in organic dyes-doped gel films. Another approach which is based on the time-independent wave equations for the random gain media can go beyond the diffusive description [7–11], but is useful only in determining the lasing threshold [12]. To fully understand the random lasing system, we have to deal with time-dependent wave equations in random systems by coupling Maxwell's equations with the rate equations of electron population within a semiclassical [13,14] theory.

In this paper, we introduce a model by combining these semiclassical laser theories with Maxwell's equations. By incorporating a well-established FDTD (finite-difference time-domain) [15] method we calculate the wave propagation in random media with gain. Because this model couples electronic number equations at different levels

with field equations, the amplification is nonlinear and saturated, so stable state solutions can be obtained after a long relaxation time. The advantages of this FDTD model are obvious, since one can follow the evolution of the electric field and electron numbers inside the system. From the field distribution inside the system, one can clearly distinguish the localized modes from the extended ones. One can also examine the time dependence of the electric field inside and just outside the system. Then after Fourier transformation, the emission spectra and the modes inside the system can be obtained.

Our system is essentially a one-dimensional simplification of the real experiments [2,3]. It consists of many dielectric layers of real dielectric constant of fixed thickness, sandwiched between two surfaces, with the spacing between the dielectric layers filled with gain media (such as the solution of dye molecules). The distance between the neighboring dielectric layers is assumed to be a random variable. The overall length of the system is L .

Our results can be summarized as follows: (i) As expected for periodic and *short* ($L < \xi$, ξ is the localization length) random system, an extended mode dominates the field and the spectra. (ii) For either strong disorder or the long ($L \gg \xi$) system, we obtain a low threshold value for lasing. By increasing the length or the gain more peaks appear in the spectra. By examining the field distribution inside the system, one can clearly see that these lasing peaks are coming from localized modes. (iii) When the gain or the pumping intensity increases even further, the number of lasing modes do not increase further, but saturate to a constant value, which is proportional to the length of system for a given randomness. And (iv) the emission spectra are not the same for different output directions which show that the emission is not isotropic. These findings are in agreement with recent experiments [2] and also make new predictions. We want to point out that our model is 1D unlike the experiments which are done in 3D samples. However, the experimental results are strongly dependent on the shape of the excitation area [2]. Sharp lasing peaks are observed when the excitation area is

stripelike, which is close to our 1D model. In the 1D case we expect the number of lasing modes to be less than the 3D case but much sharper. This is due to the fact that the modes are more localized and there are fewer propagating paths in 1D.

The binary layers of the system are made of dielectric materials with dielectric constants of $\epsilon_1 = \epsilon_0$ and $\epsilon_2 = 4 \times \epsilon_0$, respectively. The thickness of the first layer, which simulates the gain medium, is a random variable $a_n = a_0(1 + W\gamma)$ where $a_0 = 300$ nm, W is the strength of randomness, and γ is a random value in the range $[-0.5, 0.5]$. The thickness of the second layer, which simulates the scatterers, is a constant $b = 180$ nm. In the layers representing the gain medium, there is a four-level electronic material mixed inside. An external mechanism pumps electrons from ground level (N_0) to third level (N_3) at a certain pumping rate P_r , which is proportional to the pumping intensity in experiments. After a short lifetime τ_{32} , electrons can nonradiative transfer to the second level (N_2). The second level (N_2) and the first level (N_1) are called the upper and the lower lasing levels. Electrons can be transferred from the upper to the lower level by both spontaneous and stimulated emission. At last, electrons can nonradiative transfer from the first level (N_1) back to the ground level (N_0). The lifetimes and energies of upper and lower lasing levels are τ_{21} , E_2 and τ_{10} , E_1 , respectively. The center frequency of radiation is $\omega_a = (E_2 - E_1)/\hbar$, which is chosen to be equal to $2\pi \times 6 \cdot 10^{14}$ Hz. Based on real laser dyes [16], the parameters τ_{32} , τ_{21} , and τ_{10} are chosen to be 1×10^{-13} s, 1×10^{-9} s, and 1×10^{-11} s. The total electron density $N_0^0 = N_0 + N_1 + N_2 + N_3$ and the pump rate P_r are the controlled variables according to the experiments [2].

The time-dependent Maxwell equations are given by $\nabla \times \mathbf{E} = -\partial \mathbf{B}/\partial t$ and $\nabla \times \mathbf{H} = \epsilon \partial \mathbf{E}/\partial t + \partial \mathbf{P}/\partial t$, where $\mathbf{B} = \mu \mathbf{H}$ and \mathbf{P} is the electric polarization density from which the amplification or gain can be obtained. Following the single electron case, one can show [14] that the polarization density $P(x, t)$ in the presence of an electric field obeys the following equation of motion:

$$\frac{d^2 P(t)}{dt^2} + \Delta \omega_a \frac{dP(t)}{dt} + \omega_a^2 P(t) = \frac{\gamma_r}{\gamma_c} \frac{e^2}{m} \Delta N(t) E(t), \quad (1)$$

where $\Delta \omega_a = 1/\tau_{21} + 2/T_2$ is the full width at half maximum linewidth of the atomic transition. T_2 is the mean time between dephasing events which is taken to be 2.18×10^{-14} s, $\Delta N(x, t) = N_1(x, t) - N_2(x, t)$ and $\gamma_r = 1/\tau_{21}$ is the real decay rate of the second level, and $\gamma_c = \frac{e^2}{m} \frac{\omega_a^2}{6\pi\epsilon_0 c^3}$ is the classical rate. It is easy to derive [14] from Eq. (1) that the amplification line shape is Lorentzian and homogeneously broadened. Equation (1) can be thought of as a quantum mechanically correct equation for the induced polarization density $P(x, t)$ in a real atomic system.

The equations giving the number of electrons on every level can be expressed as follows:

$$\begin{aligned} \frac{dN_3(x, t)}{dt} &= P_r N_0(x, t) - \frac{N_3(x, t)}{\tau_{32}} \\ \frac{dN_2(x, t)}{dt} &= \frac{N_3(x, t)}{\tau_{32}} + \frac{E(x, t)}{\hbar \omega_a} \frac{dP(x, t)}{dt} - \frac{N_2(x, t)}{\tau_{21}} \\ \frac{dN_1(x, t)}{dt} &= \frac{N_2(x, t)}{\tau_{21}} - \frac{E(x, t)}{\hbar \omega_a} \frac{dP(x, t)}{dt} - \frac{N_1(x, t)}{\tau_{10}} \\ \frac{dN_0(x, t)}{dt} &= \frac{N_1(x, t)}{\tau_{10}} - P_r N_0(x, t), \end{aligned} \quad (2)$$

where $\frac{E(x, t)}{\hbar \omega_a} \frac{dP(x, t)}{dt}$ is the induced radiation rate or excitation rate depending on its sign.

To excite the system, we must introduce sources into the system [17]. To simulate the real laser system, we introduce sources homogeneously distributed in the system to simulate the spontaneous emission. We make sure that the distance between the two sources L_s is smaller than the localization length ξ . Each source generates waves of a Lorentzian frequency distribution centered around ω_a , with its amplitude depending on N_2 . In real lasers, the spontaneous emission is the most fundamental noise [13,14], but generally submerged in other technical noises which are much larger. In our system, the simulated spontaneous emission is the *only* noise present, and is treated self-consistently. This is the reason for the small background in the emission spectra shown below.

There are two leads, both with a width of 300 nm, at the right and the left sides of the system, and at the end of the leads we use the Liao method [15] to impose absorbing-boundary conditions (ABC). In the FDTD calculation, we discretize both the space and time. The discrete time step and space steps are chosen to be 10^{-17} s and 10^{-9} m, respectively. In the FDTD scheme the boundary conditions for the field at the interfaces between the two media are automatically satisfied, since we are numerically solving Maxwell's equations. So for a given random configuration, based on the previous time steps we can calculate the next time step ($n + 1$ step) values. First we obtain the $n + 1$ time step of the electric polarization density P by using Eq. (1), then the $n + 1$ step of the electric and magnetic fields are obtained by Maxwell's equations, and at last the $n + 1$ step of the electron numbers at each level are calculated by Eq. (2). The initial state is that all electrons are on the ground state, so there is no field, no polarization, and no spontaneous emission. Then the electrons are pumped and the system begins to evolve according to the above equations.

We have performed numerical simulations for periodic and random systems. First, for all the systems, a well-defined lasing threshold exists. As expected, when the randomness becomes stronger, the threshold intensity decreases because localization effects make the paths of waves propagating inside the gain medium much longer.

For a periodic or *short* ($L < \xi$) random system, generally only one mode dominates the whole system even if the gain increases far above the threshold. This is due to the fact that the first mode can extend in the whole system, and its strong electric field can force almost all the electrons of the upper level N_2 to jump down to the N_1 level quickly by stimulated emission. This leaves very few upper electrons for stimulated emission of the other modes. In other words, all the other modes are suppressed by the first lasing mode even though their threshold values are only a little bit smaller than the first one. This phenomenon also exists in common homogeneously broadening lasers [13].

For *long* ($L \gg \xi$) random systems, richer behavior is observed. First we find that all the lasing modes are localized and stable around their localization centers after a long time. Each mode has its own specific frequency and corresponds to a peak in the spectrum inside the system. When the gain increases beyond the threshold, the electric field pattern (see Fig. 1a) shows that more localized lasing modes appear in the system and the spectrum intensity I_e inside the system (see Fig. 1d) gives more sharp peaks just as observed in the experiments [2]. Notice that N_2 is small (Fig. 2b) in the position where the amplitude of the

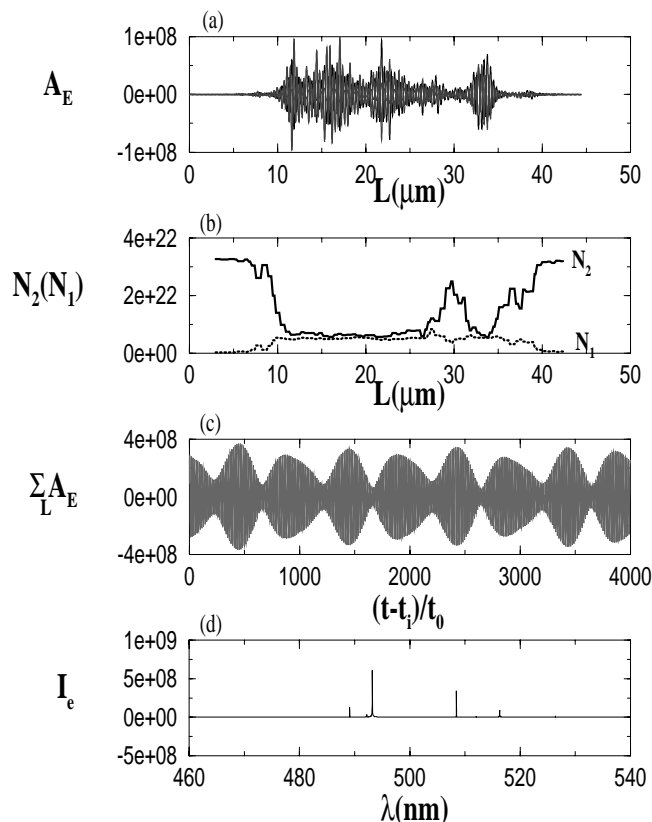


FIG. 1. (a) The amplitude of the electric field A_E in units of V/m vs the position L in the system, (b) the density of electrons in the $N_2(N_1)$ in units of $1/m^3$ levels vs L , (c) A_E in units of V/m average over length vs $(t - t_i)/t_0$, where $t_0 = 2.78 \times 10^{-17}$ s and $t_i = 7 \times 10^{-10}$ s, and (d) the spectra I_e in units of V/m vs the wavelength for a 80 cell system with $W = 1.4$, $N_0^0 = 5.5 \times 6.02 \times 10^{23} \text{ m}^{-3}$, and $P_r = 1 \times 10^7 \text{ s}^{-1}$.

electric field A_E (Fig. 1a) is large, and this is because of the stimulated emission. In Fig. 1c, the time dependence of the averaged A_E over all the spatial points is shown. I_e is obtained by taking the Fourier transform of the spatial averaged $A_E(t)$.

The exact position of the lasing peaks depends on the random configuration. Notice that the lasing peaks are much narrower than the experimental ones [2]. This is due to the 1D nature of our model. In the present case only two escaping channels exist, so it's more difficult for the wave to get out from the system which has a higher quality factor. When the gain is really big, we find the number of lasing modes will not increase any more, so a saturated number N_m of lasing modes exists for the long random system. In Fig. 2, we plot the spectral intensity vs the wavelength for different input transitions (or equivalently pumping rates). Notice these results are in qualitative agreement with the experimental results shown in Fig. 2 of the paper of Cao *et al.* [2].

These multilasing peaks and the saturated-mode-number phenomena are due to the interplay between localization and amplification. Localization makes the lasing mode strong around its localization center and exponentially small away from its center so that it only suppresses the modes in this area by reducing N_2 . When a mode lases, only those modes which are *far enough* from this mode can lase afterwards. So more than one mode can appear for a long system and each mode seems to *repel* each other. Because every lasing mode dominates a certain area and is separated from other modes, only a limited number of lasing modes can exist for a finite long system even in the case of large amplification. We therefore expect that the number of surviving lasing modes N_m should

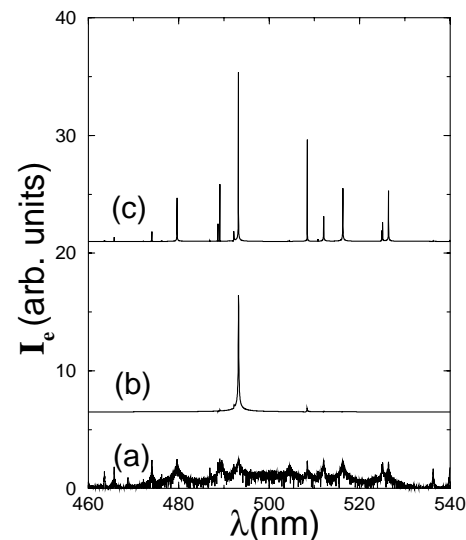


FIG. 2. The spectral intensity in arbitrary units vs the wavelength for the 80 cell system with $W = 1.4$ for different pumping rates P_r . P_r in units of s^{-1} is (a) 10^4 , (b) 10^6 , and (c) 10^{10} . To be able to plot all the curves in one figure, we have multiplied (a), (b), and (c) by 10^{-3} , 10^{-6} , and 10^{-8} , respectively, and shifted them apart.

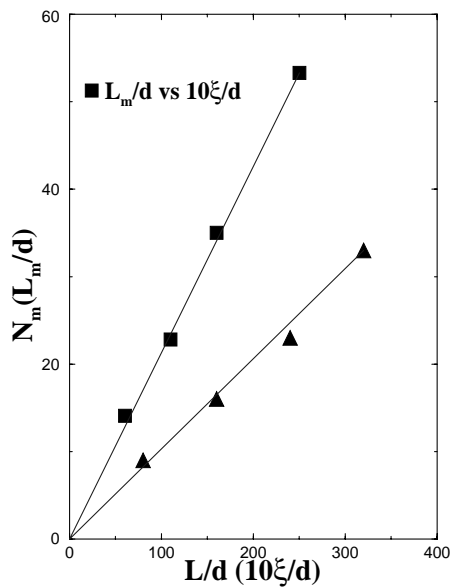


FIG. 3. The number of modes N_m vs the length of the system L/d , where $d = \langle a_n \rangle + b = 480$ nm is the size of the cell. Also the average mode length L_m/d vs the localization length $10 \times \xi/d$ for different disorder strength W for a 320 cell system. $P_r = 1 \times 10^9$ and the rest of the parameters are the same as the ones of Fig. 1.

be proportional to the length of the system L when the amplification is very large. Since the “mode-repulsion” property is coming from the localization of the modes, we expect that the average mode length $L_m = L/N_m$ should be proportional to localization length ξ too. In Fig. 3, we plot N_m vs the length of the systems L when we increase the length from 80 cells to 320 cells and keep all other parameters the same. In Fig. 3, we also plot the average mode length L_m vs the localization length ξ when we change the random strength W for a 320 cell system. The localization lengths are calculated using the transfer-matrix method by averaging 10 000 random configurations. These results confirm that indeed $N_m \propto L$ and $L_m \propto \xi$. It will be very interesting if these predictions can be checked experimentally.

The emission spectra at the right and left side of the system are quite different. This can be explained from the field pattern shown in Fig. 1a. Notice the localized modes are not similar at both sides of the system. This is the reason for this difference in the output spectrum.

The nonisotropic output spectra of real 3D experiments [2] might be explained by assuming that every localized mode has its intrinsic direction, strength, and position, and the detected output spectra in experiments at different directions are the overlap of contributions from many modes. So generally they should be different.

In summary, by using a FDTD method we constructed a random lasing model to study the interplay of localization and amplification. Unlike the time-independent models, the present formulation calculates the field evolution beyond the threshold amplification. This model allows us to obtain the field pattern and spectra of localized lasing

modes inside the system. For random systems, we can explain the multi-peaks and the nonisotropic properties in the emission spectra, seen experimentally. Our numerical results predict the mode-repulsion property, the lasing-mode saturated number, and average mode length. We also observed the exchange of energy between the localized modes which is much different from common lasers and this is essential for further research of mode competition and evolution in random laser.

Ames Laboratory is operated for the U.S. Department of Energy by Iowa State University under Contract No. W-7405-Eng-82. This work was supported by the director for Energy Research, Office of Basic Energy Sciences.

-
- [1] V. S. Letokhov, *Sov. Phys. JETP* **26**, 835 (1968).
 - [2] H. Cao, Y. G. Zhao, S. T. Ho, E. W. Seelig, Q. H. Wang, and R. P. H. Chang, *Phys. Rev. Lett.* **82**, 2278 (1999); S. V. Frolov, Z. V. Vardeny, K. Yoshino, A. Zakhidov, and R. H. Baughman, *Phys. Rev. B* **59**, 5284 (1999).
 - [3] N. M. Lawandy, R. M. Balachandran, S. S. Gomers, and E. Sauvain, *Nature (London)* **368**, 436 (1994).
 - [4] D. S. Wiersma, M. P. van Albada, and Ad Lagendijk, *Phys. Rev. Lett.* **75**, 1739 (1995); D. S. Wiersma *et al.*, *Phys. Rev. E* **54**, 4256 (1996).
 - [5] A. Yu. Zyuzin, *Phys. Rev. E* **51**, 5274 (1995).
 - [6] S. John and G. Pang, *Phys. Rev. A* **54**, 3642 (1996), and references therein.
 - [7] Qiming Li, K. M. Ho, and C. M. Soukoulis (unpublished).
 - [8] P. Pradhan and N. Kumar, *Phys. Rev. B* **50**, 9644 (1994).
 - [9] Z. Q. Zhang, *Phys. Rev. B* **52**, 7960 (1995).
 - [10] J. C. J. Paasschens, T. Sh. Misirpashaev, and C. W. J. Beenakker, *Phys. Rev. B* **54**, 11 887 (1996).
 - [11] Xunya Jiang and C. M. Soukoulis, *Phys. Rev. B* **59**, 6159 (1999).
 - [12] Xunya Jiang, Qiming Li, and C. M. Soukoulis, *Phys. Rev. B* **59**, R9007 (1999).
 - [13] A. Maitland and M. H. Dunn, *Laser Physics* (North-Holland Publishing Company, Amsterdam, 1969). See Chaps. 3, 8, and 9.
 - [14] Anthony E. Siegman, *Lasers* (Mill Valley, California, 1986). See Chaps. 2, 3, 6, and 13.
 - [15] A. Taflove, *Computational Electrodynamics: The Finite-Difference Time-Domain Method* (Artech House, London, 1995). See Chaps. 3, 6, and 7.
 - [16] Such as the coumarine 102 or uranin with meth as solvent. Our results are of general validity and are not sensitive to the lasing dyes used.
 - [17] The structure of our 1D random medium is an alternate of layers of random thickness representing the gain medium and dielectric layers of constant thickness representing the scatterers. Theoretically, every discrete grid point of the layers representing the gain medium, is a source that can generate spontaneous emission. Because this is very time consuming, we selected to use a finite number (20 to 50) of sources. To simulate real spontaneous emission, every source needs a proper vibration amplitude and a Lorentzian frequency distribution. We have checked that the spatial distribution of the sources does not influence the calculation results.